Am J Transl Res 2022;14(10):7552-7565
www.ajtr.org /ISSN:1943-8141/AJTR0145285

Original Article

STAT3 signaling mediates peritoneal fibrosis by activating hyperglycolysis

Jiao Fu[1], Nan Li[1], Mengmeng He[1], Dake Huang[2], Pei Zhang[1]

[1]*Department of Nephrology, The First Affiliated Hospital of Anhui Medical University, Hefei 230032, Anhui, P.R. China;* [2]*Synthetic Laboratory of Basic Medicine College, Anhui Medical University, Hefei 230032, Anhui, P.R. China*

Received July 12, 2022; Accepted September 30, 2022; Epub October 15, 2022; Published October 30, 2022

Abstract: Background: Long term peritoneal dialysis leads to peritoneal epithelial-mesenchymal transformation (EMT), angiogenesis, and ultrafiltration failure. Although recent evidence suggests that inhibiting STAT3 (signal transducer and activator of transcription 3) can prevent kidney fibrosis, and that STAT3 can enhance glucose metabolism, the effect of STAT3 in peritoneal fibrosis (PF) has not been clarified. Methods: Our study determined the effects of STAT3 on EMT and key glycolysis enzymes in mesothelial HMrSV5 cells by knockdown and overexpression of STAT3. In addition, we established a rat PF model to examine the role of pharmacologic inhibition of STAT3 or 6-phosphofructo-2-kinase/fructose-2, 6-bisphosphatase 3 (PFKFB3) in this process. Results: High glucose (HG) caused the upregulation of α-smooth muscle actin and transforming growth factor beta 1 and the downregulation of E-cadherin, and induced STAT3 activation in HMrSV5 cells. In addition, HMrSV5 cells cultured in high glucose showed high expression of key glycolysis enzymes, which could be inhibited by STAT3 siRNA. Furthermore, treating mesothelial cells with 3PO, the PFKFB3 inhibitor, could attenuate high glucose-induced EMT. Moreover, daily administration of dialysis fluid could induce peritoneal fibrosis. The peritoneal fibrosis was accompanied by enhanced phosphorylation of STAT3 and the upregulation of PFKFB3. The administration of BP-1-102 or 3PO prevented fibrosis and inhibited angiogenesis in PF rats. Conclusions: si-STAT3 attenuated the HG-induced EMT and hyperglycolysis, and the overexpression of STAT3 could induce EMT in HMrSV5 cells. 3PO could markedly attenuate HG-induced EMT by decreasing PFKEB3 in HMrSV5 cells. In addition, we demonstrated that inhibiting STAT3 signaling or peritoneal hyperglycolysis could attenuate peritoneal fibrosis and angiogenesis in vivo. Our findings linked the STAT3/PFKFB3 signaling to the development of PF. HG/STAT3/PFKFB3 might promote the progression of PF through regulating profibrosis and angiogenesis.

Keywords: STAT3, PFKFB3, hyperglycolysis, peritoneal fibrosis, EMT

Introduction

Peritoneal dialysis (PD) is an effective therapeutic modality for patients with end-stage renal disease (ESRD) and is increasingly utilized globally. Peritoneal fibrosis (PF) is the most common complication of PD. PF is usually manifested as a structural disruption of the peritoneum and irreversible damage to the functional integrity of the peritoneum. PF is thought to be the response to various injuries including uremic toxins, peritonitis, and damage caused by bioincompatible dialysate (low pH, hyperglucose and glucose degradation products) [1]. Among these risk factors, EMT, pro-inflammatory and neo-angiogenesis processes mediated by HG-PDF (high glucose peritoneal dialysis fluid) are key to causing changes in the function and structure of the peritoneum [2]. Moreover, an increase in the peritoneal small solute transport rate (PSTR) in the peritoneum results in impaired ultrafiltration. The alteration of peritoneal structure and the loss of ultrafiltration function eventually lead to the progressive development of PF and prevent patients from undergoing PD [3, 4]. Therefore, it is important to understand the mechanism driving PF development and identify more effective preventive strategies. Blocking autophagy, targeting Toll-like receptors, or inhibiting hyperglycolysis in mesothelial cells have been discovered to prevent PF in recent years [5-7]; howev-

er, the detailed underlying mechanism of PF occurrence still remains to be fully understood.

STAT3, a key signaling protein, responds to many cytokines and growth factors to trigger different biological outcomes [8, 9]. Recent evidence suggests that inhibiting the activation of STAT3 prevents fibrosis [10-13]. Inhibiting STAT3 prevents STZ-induced kidney fibrosis and nephropathy [10, 14], and the S3I-201 (STAT3 inhibitor) can suppress liver fibrosis and angiogenesis by inhibiting STAT3 [15-17]. Consistent with this, STAT3 signaling has been found to be activated in HG-PDF-induced PF mouse models and in high glucose-stimulated mesothelial cells. Furthermore, inhibiting STAT3 could prevent EMT in mesothelial cells and ultimately suppress PF [18]. Our previous studies have found that STAT3 inhibitor (BP-1-102) attenuate EMT in HMrSV5 cells by downregulating TGF-β1 (transforming growth factor beta 1) expression and restraining the level of AGEs (advanced glycation end products) and MGO (methylglyoxal) [19]. BP-1-102 is a novel STAT3 inhibitor that inhibits STAT3 with a high affinity. However, the effect of inhibiting STAT3 on PF in vivo remains unclear.

At the molecular level, STAT3 was reported to induce expression of various genes [20-22]. In renal tubular epithelial cells, S3I-201 could downregulate the high glucose-induced TGF-β1, VEGF, AT1, and ACE [10]. Interleukin (IL)-6 activated STAT3 also enhances expression of the glycolytic enzymes hexokinase 2 (HK2) and PFKFB3. HK2 and PFKFB3 are key rate-limiting enzymes in glycolysis, as ectopic expression of PFKFB3 enhances glycolysis [23]. Furthermore, PFKFB3-dependent glycolysis is an essential feature required to induce the activation of a fibrogenic phenotype during hepatic stellate cell (HSC) activation. PFKFB3 blockade impairs these changes and reduces matrix production [24]. A study demonstrated that exposing mesenchymal cells to PD fluid resulted in excessive glycolysis, which promoted not only energy requirements but also cell phenotypic transformation and proliferation. Blocking excessive glycolysis greatly suppressed EMT in both types of mesothelial cells [7]. In this context, we conjectured that there might be a crosstalk between STAT3 activation and key glycolysis enzymes during the process of EMT and PF.

In the current study, we examined the role of STAT3 activation on the upregulation of glycolysis related enzymes and the EMT of HMrSV5 cells caused by HG, and the effect of blocking STAT3 or glycolysis on fibrogenesis and angiogenesis during PD. A clearly defined PFKFB3 inhibitor 3PO was used to suppress glycolysis to further demonstrate the role of glycolysis on EMT induced by HG. The purpose of this research is to investigate the participation of the STAT3/PFKFB3 pathway in the process of PF using HMrSV5 cells and PF rat models.

Materials and methods

Reagents

Antibodies: p-STAT3 (CST, #9145), E-cadherin (Affinity, #AF0131), α-SMA (α-smooth muscle actin) (Affinity, #AF1032), VEGFR2 (vascular endothelial growth factor receptor 2) (Affinity, #AF6218), TGF-β1 (Affinity, #AF1027), PFKFB3 (Affinity, #DF12016), PKM2 (pyruvate kinase M2) (Affinity, #AF5234), LDHA (lactate dehydrogenase A) (Affinity, #DF6280), STAT3 (CST, #9139), β-actin (Affinity, #AF7018). Fetal bovine serum (FCS) and Modified Eagle Medium (MEM) were obtained from Gibco. Glucose was purchased from Sigma. Both BP-1-102 (S7769) and 3PO (S7639) were purchased from Selleck (Shanghai, China).

Cell culture

HMrSV5 cells were obtained from Zhongshan University and cultured in MEM medium under 37°C humidifying incubator with 5% CO_2. The MEM medium contained 10% FCS and 1% penicillin/streptomycin solution (Beyotime). To mimic the HG-PDF environment in vitro, glucose was supplemented to MEM. The concentration of glucose in the MEM medium reached 84 mM, 138 mM, and 236 mM, equal to hypertonic peritoneal dialysis solution (Dianeal 1.5%, Dianeal 2.5% and Dianeal 4.25%) currently used for PD in clinic.

Cell viability assay

Briefly, HMrSV5 cells were seeded into a 96-well plate. After 24 hours' culture, the cells were treated with vehicle or different concentrations of test compounds for 24 h. After adding 20 μL MTT solution 3-(4,5-Dimethylthiazol-2-yl)-2,5-diphenyltetrazolium bromide to each

Table 1. Sequences of primers

Gene	Forward (5'-3')	Reverse (5'-3')
Human STAT3	ATCACGCCTTCTACAGACTGC	CATCCTGGAGATTCTCTACCACT
Human PFKFB3	AGCCCGGATTACAAAGACTGC	GGTAGCTGGCTTCATAGCAAC
Human PKM2	ATAACGCCTACATGGAAAAGTGT	TAAGCCCATCATCCACGTAGA
Human LDHA	ATGGCAACTCTAAAGGATCAGC	CCAACCCCAACAACTGTAATCT
Human E-cadherin	AAAGGCCCATTTCCTAAAAACCT	TGCGTTCTCTATCCAGAGGCT
Human TGF-β1	CAATTCCTGGCGATACCTCAG	GCACAACTCCGGTGACATCAA
Human α-SMA	AAAAGACAGCTACGTGGGTGA	GCCATGTTCTATCGGGTACTTC
Human β-actin	CCCTGGAGAAGAGCTACGAG	GGAAGGAAGGCTGGAAGAGT
Rat PFKFB3	CACGGCGAGAATGAGTACAA	TTCAGCTGACTGGTCCACAC
Rat STAT3	TATCTTGGCCCTTTGGAATG	GTGGGGATACCAGGATGTTG
Rat β-actin	TGTCACCAACTGGGACGATA	GGGGTGTTGAAGGTCTCAAA

well for 4 h, 150 μL DMSO (Dimethyl Sulphoxide) was added to each well. The optical density (OD) was measured by the microplate reader (Multiskan MK3) at the wavelength of 490 nm, and the cell viability relative to the control cells was determined by the absorbance.

Mesothelial cell transfection

Silencing and overexpressing of gene expression was achieved by STAT3 siRNA and STAT3 plasmid respectively. The gene-specific siRNAs and STAT3 plasmid were purchased from GenePharma (Shanghai, China). The STAT3 siRNA and STAT3 plasmid were transiently transfected into HMrSV5 cells by Lipofectamine 2000 (Invitrogen, CA, USA). After 48 h, the overexpression and knockdown efficiency of STAT3 were measured using real-time PCR and western blot analysis.

The specific target sequences of siRNAs were as follows: STAT3: sense, 5'-GGUACAUCAUGGGCUUUAUTT-3', antisense, 5'-AUAAAGCCCAUGAUGUACCTT-3'. Control: sense, 5'-UUCUCCGAACGUGUCACGUTT-3', antisense, 5'-ACGUGACACGUUCGGAGAATT-3'.

Reverse transcription and real-time quantitative PCR

TRIZOL (Invitrogen, Carlsbad, CA) was used to isolate total RNA from cells and tissues. Then, the total RNA was reverse-transcribed to cDNA using a reverse transcriptome. Real-time PCR assay was performed with Hieff qPCR SYBR Green Master Mix (Yeasen Biotech) by CFX96 real-time PCR system (Bio-Rad, CA). Primers, shown in **Table 1**, were obtained from Sangon Biotech (Shanghai, China). The relative changes of mRNA were standardized to housekeeping gene β-actin and calculated by $2^{-\Delta\Delta Ct}$.

HG-PDF-induced PF rat model

The animal protocol was approved by the Ethics Committee of Animal Research of Anhui Medical University (No: LLSC20211055). The male SD rats (8 to 10 weeks) were kept in cages under SPF (specific pathogen-free) conditions. Rats were separated into five groups randomly (n = 6): sham group, normal saline (NS) group, PF group, BP-1-102 group and 3PO group. A catheter (Solomon Scientific) was implanted under the skin on the back of the animal with the tip positioned within the peritoneal membrane [25, 26]. In the NS group, the abdominal cavity of each rat was respectively injected in 10 ml 0.9% normal saline every morning and night. An equal volume of PDF solution (Dianeal 4.25%) was injected into the rats in PF group. To explore the effects of STAT3 and glycolysis on PF, the rats were administered intraperitoneally daily with BP-1-102 (1 mg/kg) or 3PO (20 mg/kg) in 10 ml PDF as recommended by the manufacturer in the BP-1-102 group and the 3PO group respectively. After treatment for 10 weeks, the peritoneal dialysis effluent was collected for peritoneal equilibration test (PET) before euthanizing the rats, and tissue samples were collected for further analysis.

Peritoneal equilibration test (PET)

Before the rats were euthanized, 20 mL of Dianeal 4.25% was injected into the abdominal cavity of each rat to estimate the peritoneal membrane transport function [27]. After 90 minutes, the remaining dialysate in rat abdominal cavity was completely drained and collected. The peritoneal transport function was determined by the ratio between the glucose concentration in dialysate at 90 minutes post injection and the initial dialysate glucose con-

centration (D90/D0). The levels of inflammatory factors were measured in the peritoneal dialysis effluent.

Histologic analysis of the peritoneum

Standard protocol was followed for histological analysis. Briefly, after fixing and embedding in paraffin, peritonea were cut into 3 μm thick sections and mounted on slides. For histological analysis, the slides were deparaffinized, rehydrated and stained by H&E and Masson trichrome staining. In addition, VEGFR2 (Affinity, #AF6218) and TGF-β1 (Affinity, #AF1027) were the primary antibodies used for immunochemistry. After deparaffinizing and rehydrating, the slides were treated with the endogenous peroxidase blocker (OriGene Tech) at 37°C for 15 minutes. Next, the slides were immersed into citrate solution in a pressure cooker and heated for 3 minutes for antigen retrieval followed by blocking at 37°C with 10% goat serum for 15 min. After incubating primary antibody (1:100 dilution) overnight at 4°C, the slides were incubated in company with the secondary antibody. Then, the slides were counterstained with hematoxylin after signal development with 3,3'-Diaminobenzidine (DAB). Finally, Leica DM6B (an upright fluorescence microscope) was used to examine the slides.

Western blot analysis

RIPA buffer supplemented with 2% ethylenediaminetetraacetic acid (EDTA, Beyotime), 2% phosphatase inhibitor and 2% protease inhibitor were used to lyse cells and tissue. The protein concentration was determined by BCA Protein Assay Kit (Epizyme). Proteins were separated and transferred onto PVDF membrane (Millipore, Bedford, USA). The PVDF membrane was blocked with Protein Free Rapid Block Buffer (EpiZyme, PS108), and then were incubated with the primary antibodies against human STAT3, p-STAT3, LDHA, PFKFB3, PKM2, TGF-β1, E-cadherin (all 1:1000 dilutions), and β-actin (1:5000 dilutions) overnight at 4°C. The second day, the membrane was incubated in secondary antibody conjugated with horseradish peroxidase for 45 min at room temperature. The signals were captured by a chemiluminescent detection system (Tanon Science & Technology Co., Ltd). Finally, the data were analyzed by Image J for Windows 64 and normalized against β-actin.

Statistical analyses

Each experiment was conducted independently three times. Data were expressed as mean ± standard error (SE). One-way analysis of variance using SPSS Statistics 23.0 (IBM, Armonk, NY, USA) determined the statistical significance of differences among groups. $P < 0.05$ indicated a significant difference.

Results

Activation of STAT3 and Upregulation of PFKFB3 in a rat PF model

We developed a rat PF model by injecting HG-PDF to SD rats for 10 weeks. In PF rats, we found a thickened subperitoneal region and the deposition of collagen fibers in rat peritoneum, as detected by Masson's trichrome staining (**Figure 1A**, **1C**). Consistent with these results, immunohistochemical staining revealed that TGF-β1 expression was increased in the subperitoneal region in the PF group (**Figure 1B**, **1D**). We detected the upregulation of STAT3 mRNA and PFKFB3 mRNA in PF rats by real-time PCR (**Figure 1E**, **1F**). In addition, we observed the upregulation of PFKFB3 and the activation of STAT3 in the fibrotic peritoneal tissues by western blot analysis (**Figure 1G**, **1H**).

Effect of HG-PDF on angiogenesis and functional changes in PF rats

Furthermore, PF rats exhibited thicker sub-peritoneal region with a large number of new blood vessels in the peritoneum as detected by H&E staining (**Figure 2A**, **2C**, **2D**). The increased expression of VEGFR2 in the peritoneal tissues also indicated that HG-PDF enhanced the density of blood vessels in the subperitoneal region (**Figure 2B**, **2E**). In addition, PET analysis revealed that the damage to peritoneal membrane function in the PF group was more severe than in the sham group (glucose D90/D0: 0.271±0.018 vs 0.401±0.023, $P = 0.006$; net ultrafiltration (nUF): 3.333±0.333 vs 8.000± 0.577 ml, $P = 0.002$) (**Figure 2F**, **2G**). Analysis of the drained remaining dialysate in PD rats indicated that PF was accompanied with the upregulation of Interleukin (IL)-1 (**Figure 2H**). Nevertheless, the level of Interleukin (IL)-6 was upregulated in both NS and PDF groups, while TNF-α level was similar among the three groups (**Figure 2I**, **2J**).

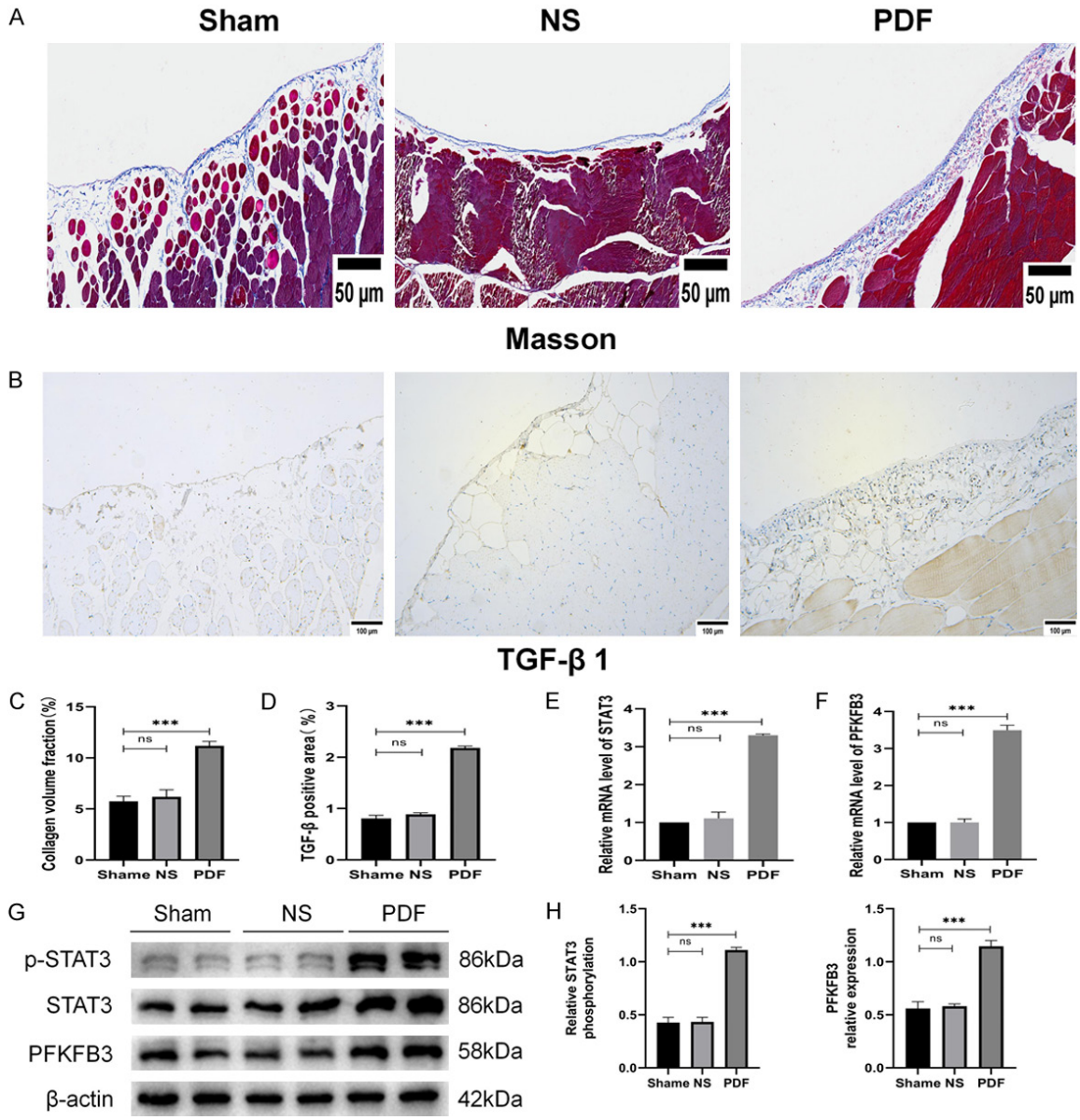

Figure 1. Activation of STAT3 and upregulation of PFKFB3 in a rat PF model. A. Images of Masson's trichrome staining. Bar = 50 μm, × 200. B. Images of immunohistochemistry staining against TGF-β1 in the submesothelial compact zone of peritoneum. Bar = 100 μm, × 100. C, D. Quantification of Masson's trichrome staining and immunostaining against TGF-β1. E, F. mRNA of STAT3 and PFKFB3 of peritoneal membrane tissue from rats. G, H. Immunoblots of p-STAT3, STAT3, PFKFB3, and β-actin. ***P < 0.001; ns, not significant. Abbreviations: NS, Normal Saline. PDF, Peritoneal Dialysis Fluid.

Activation of STAT3 in HMrSV5 cells

We investigated the activation of STAT3 in HMrSV5 cells by western blots. We discovered that STAT3 phosphorylation was induced after 48 h of HG (236 mmol/L) treatment in HMrSV5 cells (**Figure 3A**, **3B**). STAT3 phosphorylation could also be induced by lower concentrations of glucose such as 84 mM (1.5%) and 136 mM (2.5%) in HMrSV5 cells; however, the most significant phosphorylation of STAT3 was achieved by treating the cells with higher concentration of glucose (236 mM, 4.25%) (**Figure 3C**, **3D**).

HG induced EMT in HMrSV5 cells

Importantly, we discovered that different concentrations of glucose upregulated the expres-

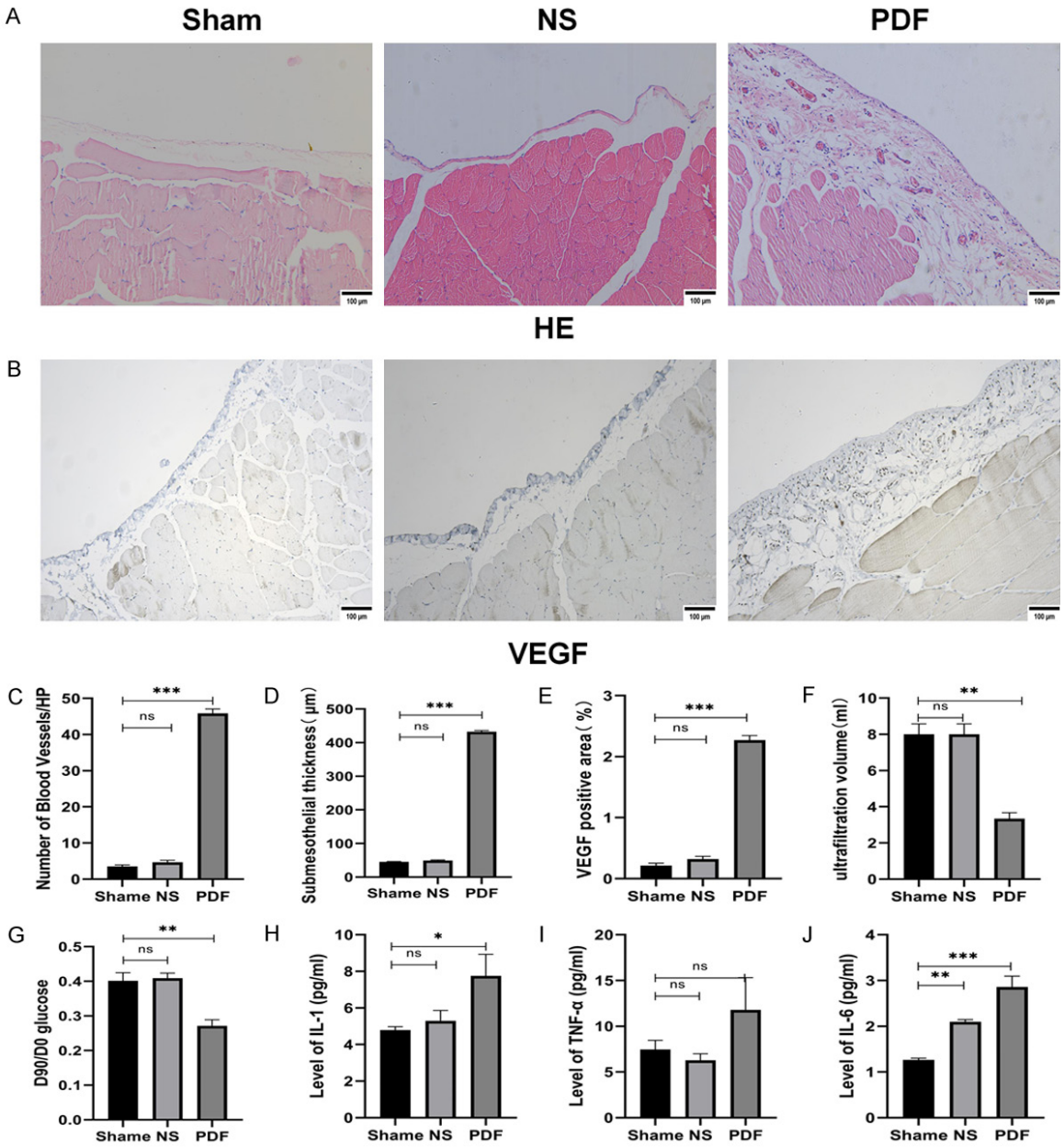

Figure 2. Effect of HG-PDF on angiogenesis and functional changes in PF rats. A, B. Images of H&E and immunohistochemical staining against VEGFR2 in the submesothelial compact zone of peritoneum. Bar = 100 μm, × 100. C. Quantitative data of the number of blood vessels of peritoneum. D. Quantitative data of the thickness in the compact zone of peritoneum. E. The quantification of immunostaining for VEGFR2. F. Quantification of ultrafiltration capacity. G. Analysis of glucose transport rates of peritoneum. H-J. Analysis of IL-1, IL-6, and TNF-α in peritoneal effluent. *P < 0.05, **P < 0.01, ***P < 0.001; ns, not significant. Abbreviations: NS, Normal Saline. PDF, Peritoneal Dialysis Fluid.

sion of TGF-β1 (fibrosis marker) and α-SMA (mesenchymal marker), but significantly downregulated the expression of E-cadherin (EMT marker) in HMrSV5 cells by western blot analysis. These effects were most pronounced in 236 mM (4.25%) glucose-treated HMrSV5 cells (**Figure 3E-H**).

Knockdown of STAT3 attenuated the HG-induced EMT and hyperglycolysis in HMrSV5 cell

To determine the functional importance of STAT3 in HG-caused EMT and hyperglycolysis in mesothelial cells, we used STAT3 siRNA to

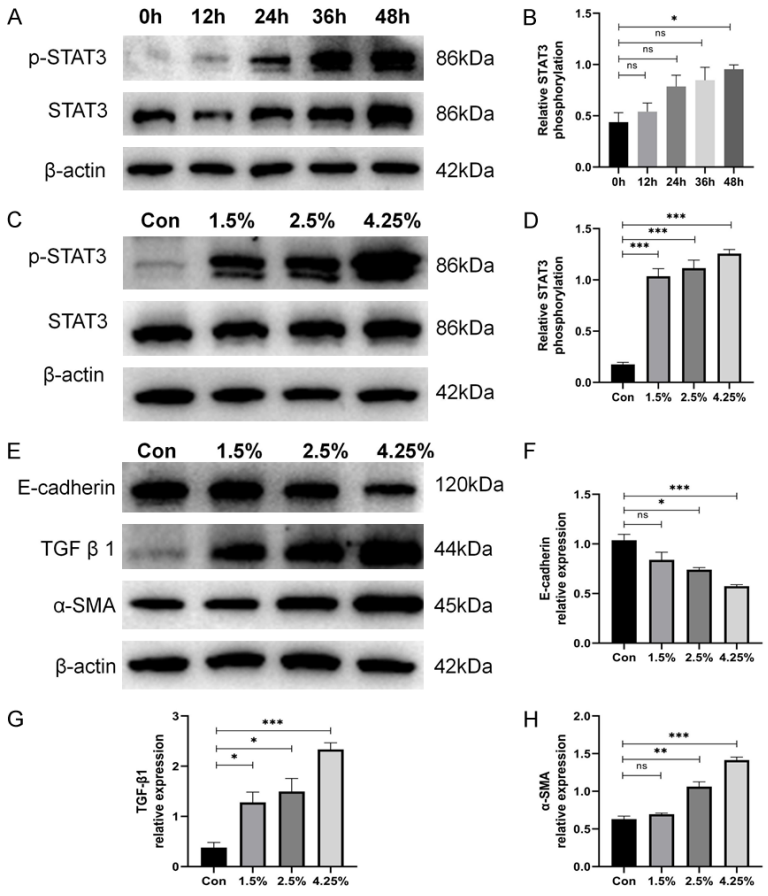

Figure 3. HG induced STAT3 activation and EMT in HMrSV5 cells. (A, B) Cells were treated with high glucose for different times (0, 12, 24, 36, 48 h) or (C, D) incubated with diverse concentrations of glucose 84 mM (1.5%), 136 mM (2.5%), 236 mM (4.25%) for 48 h. The expressions of p-STAT3 and STAT3 were detected by western blot analysis. (E-H) E-cadherin, α-SMA, and TGF-β1 were detected by western blot analysis in cells incubated with diverse concentrations of glucose. β-actin was used as a loading control. *P < 0.05; **P < 0.01; ***P < 0.001; ns, not significant. Abbreviations: con, Control.

knock down STAT3. Real-time PCR and western blot analysis confirmed the successful knockdown of STAT3. Compared to the siNC group, siSTAT3-1878 showed an obvious knockdown effect (**Figure 4A**, **4B**). siSTAT3 cells were then cultured in 236 mmol/L high glucose-containing medium for 48 h, and the mRNA level and the marker proteins level were examined by real-time PCR and western blot. We discovered that high glucose increased the level of α-SMA, TGF-β1, and the key glycolysis enzymes (PFKFB3, LDHA and PKM2), but significantly decreased the level of E-cadherin in HMrSV5 cells. However, these effects were attenuated by transfection of siSTAT3 (**Figure 4E-H**). In addition, we detected the transcriptional level by qRT-PCR, and found that siSTAT3 also reversed the mRNA of PFKFB3, LDHA, PKM2, E-cadherin, α-SMA, and TGF-β1, which were induced by high glucose (**Figure 4C**, **4D**).

Overexpressed STAT3 induced EMT in HMrSV5 cells

We overexpressed STAT3 using plasmid, and the real-time PCR results showed that overexpressed STAT3 plays a similar high glucose role in promoting EMT (**Figure 5A-C**). Western blot analysis showed that overexpressing STAT3 significantly increased α-SMA and decreased E-cadherin in HMrSV5 cells (**Figure 5D-G**).

BP-1-102 and 3PO affected the viability of HMrSV5 cells and 3PO reduced HG-caused EMT in HMrSV5 cells

The cytotoxicity of BP-1-102 and 3PO was determined by MTT method. We treated HMrSV5 cells with diverse concentrations of BP-1-102 and 3PO for 24 h and measured the cells' viability. The results showed that a low concentration of BP-1-102 (1.25-20 μM) and 3PO (1.25-10 μM) had no detectable cytotoxic effect on cell viability. Both BP-1-102 and 3PO could effectively restore the viability of HG-treated cells at a concentration of 5 μM (**Figure 6A**, **6B**). In addition, we further verified the role of 3PO on the HG-caused EMT. Western blot analysis and real-time PCR demonstrated that high glucose treatment led to an increasing α-SMA and a significantly decreasing E-cadherin. These changes were markedly attenuated after 3PO treatment (**Figure 6C-I**).

Effect of BP-1-102 or 3PO on PF rats

After injecting HG-PDF into SD rats for 10 weeks, we found that collagen fibers were deposited in the subperitoneal region with a large number of vessels in the PF rat. However, BP-1-102 or 3PO treatment reduced the densi-

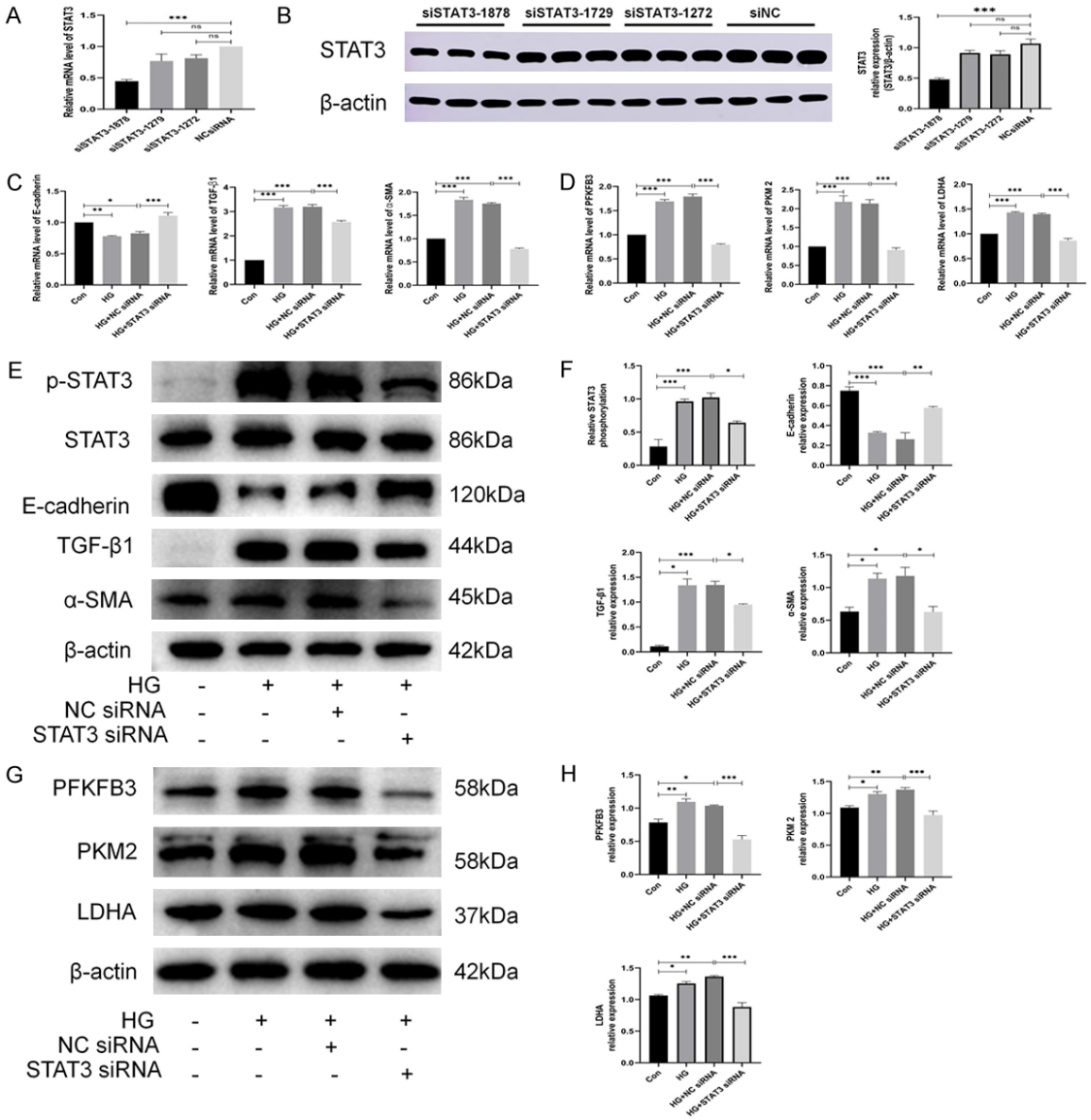

Figure 4. Knockdown of STAT3 alleviated the high glucose-induced EMT and hyperglycolysis in HMrSV5 cell. A, B. Compared to the si-NC group, si-STAT3-1878 successfully inhibited STAT3. C, D. Cells were treated with high glucose, after transfecting with siRNA or negative control. PCR showed the mRNA levels of E-cadherin, αSMA, TGF-β1, PFKFB3, PKM2 and LDHA. E, F. The expressions of STAT3, p-STAT3, α-SMA, E-cadherin and TGF-β1 were detected by western blot. G, H. The expressions of PFKFB3, PKM2 and LDHA were detected by western blot. β-actin was used as a loading control. *P < 0.05; **P < 0.01; ***P < 0.001; ns, not significant. Abbreviations: con, Control. HG, High Glucose.

ty of blood vessels and the level of collagen fibers deposited in the sub-peritoneal region (**Figure 7A**, **7B**, **7E**, **7F**). Thus, a thinner sub-peritoneal region was detected in rats with BP-1-102 group or 3PO group than in the HG-PDF group. These results were supported by the immunohistochemical staining, in which the staining of TGF-β1 and VEGFR2 was weaker in the BP-1-102 group and 3PO group than in the PF group (**Figure 7C**, **7D**, **7G**, **7H**). We further examined the effects of BP-1-102 or 3PO on peritoneal transport function in PF rats. A more significantly impaired peritoneal membrane function was found in the PF group than in the NS group. Inhibition of STAT3 by BP-1-102 elevated the glucose D90/D0 compared to the PF group (0.359±0.019 vs 0.271±0.018, P = 0.027) and nUF (5.667±0.333 vs

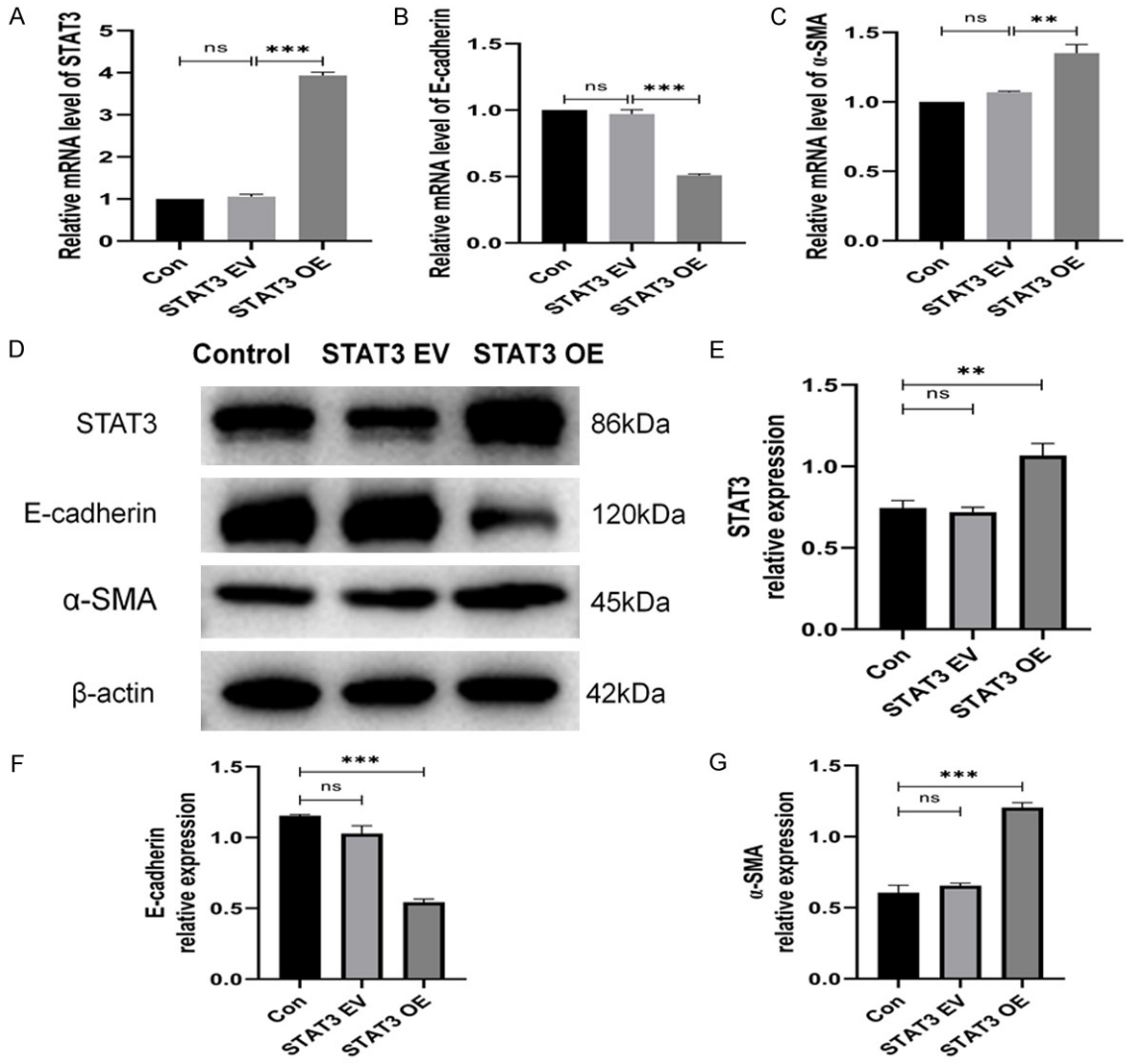

Figure 5. Overexpressed STAT3 induced EMT in HMrSV5 cells. A. The overexpression of STAT3 in normal HMrSV5 cells. B, C. The mRNA for E-cadherin and α-SMA after overexpressing STAT3. D-G. Western blot showed the expression of STAT3, α-SMA, E-cadherin after overexpressing STAT3. **P < 0.01; ***P < 0.001; ns, not significant. Abbreviations: con, Control. EV, Empty Vector. OE, Overexpression.

3.333±0.333 ml, P = 0.033). Similarly, inhibition of hyperglycolysis by 3PO increased glucose D90/D0 (0.386±0.016 vs 0.271±0.018, P = 0.006) and nUF (6.000±0.577 vs 3.333± 0.333 ml, P = 0.017) compared to the PF group (**Figure 7I**, **7J**). Hence, BP-1-102 or 3PO improved the impaired peritoneal membrane function in PF rats. Moreover, we detected the levels of inflammatory factors in drained dialysate. Compared to the HG-PDF group, IL-1 was significantly reduced in both BP-1-102 and 3PO groups (**Figure 7K**). IL-6 was reduced only in the BP-1-102-treated group, while it was not affected in 3PO-treated group (**Figure 7L**). However, neither BP-1-102 nor 3PO treatment affected the level of TNF-α (**Figure 7M**).

Discussion

Successful peritoneal dialysis (PD) therapy largely depends on the functional and structural integrity of the peritoneum. However, various unfavorable factors in long-term PD therapy can damage the function and structure of the peritoneum, thereby predisposing to PF [1].

In this study, we aim to elucidate the role of STAT3 and glycolysis in long-term PD. We found that STAT3 was activated in the HG-PDF-

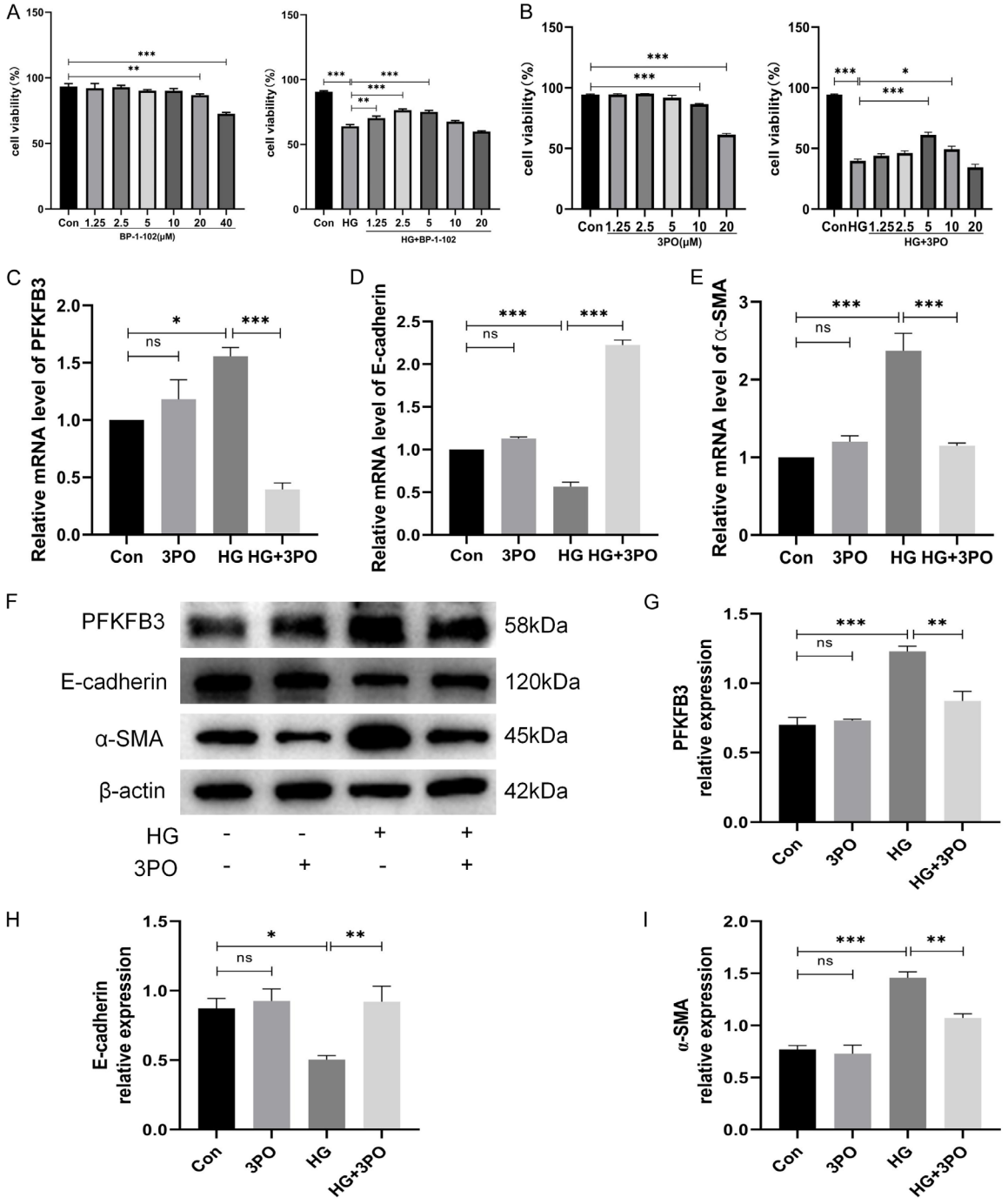

Figure 6. 3PO reduced high-glucose-induced EMT in HMrSV5 cells. A, B. Cells were treated with BP-1-102 or 3PO (1.25-20 μM) for 24 h and then assessed by MTT. C-E. The mRNA level of PFKFB3, α-SMA and E-cadherin in HG-induced HMrSV5 cells with or without 3PO treatment. F-I. The expression level of PFKFB3, α-SMA, and E-cadherin. *P < 0.05; **P < 0.01; ***P < 0.001; ns, not significant. Abbreviations: con, Control. HG, High Glucose.

induced rat PF model, consistent with upregulation of phosphorylated STAT3 in patients with long-term PD [18, 28]. Then we performed H&E, and Masson staining showed the accumulation of collagen fibers and the thickening of the subcutaneous region in the peritoneal tissues from PF rats. The immunohistochemical staining also revealed increasing TGF-β1 and VEGFR2 in the subperitoneal region of PF rats. These changes were identical to the key patho-

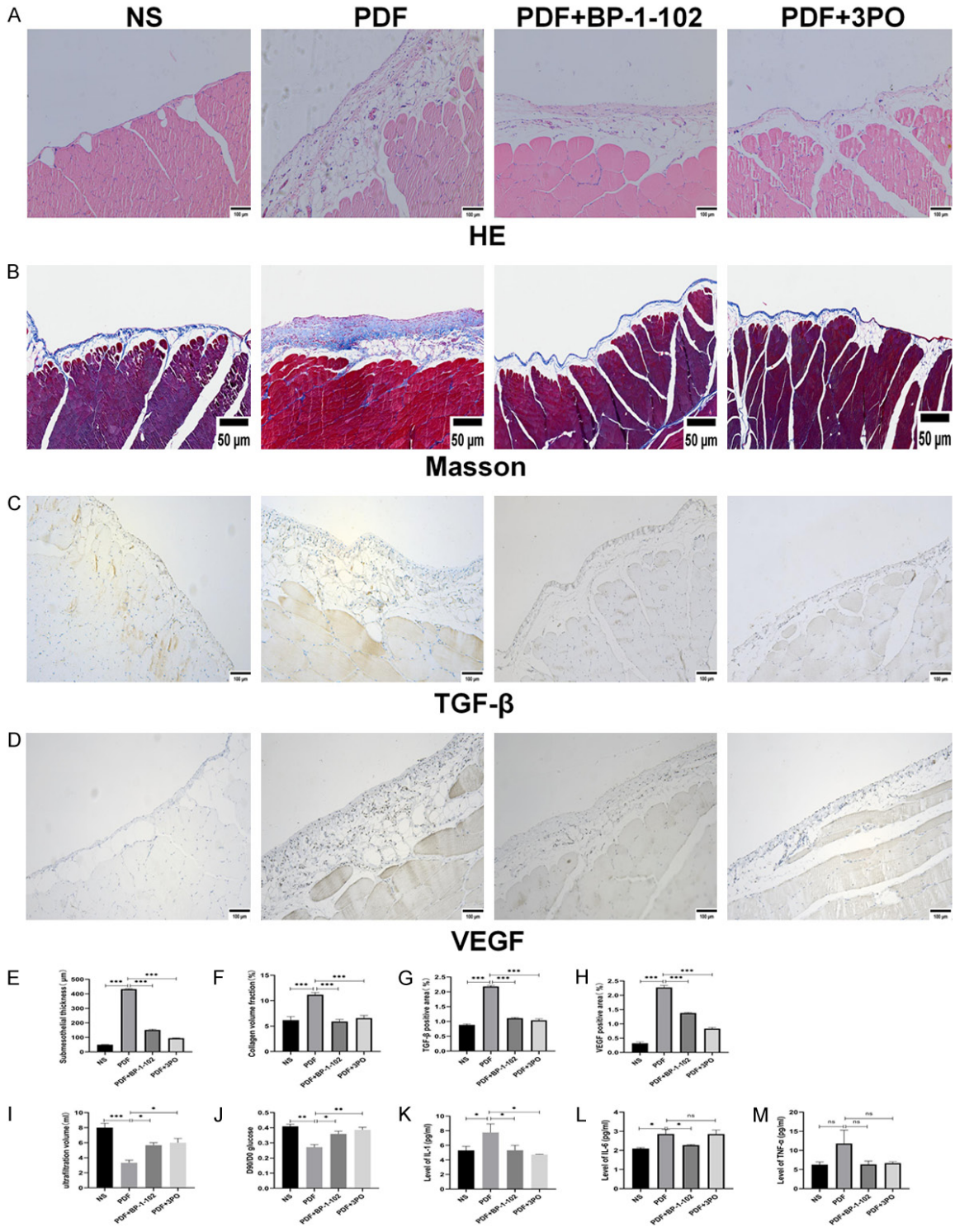

Figure 7. Changes in peritoneal histopathology in the four experimental groups showing the effects of BP-1-102 or 3PO in PF rats. A, C, D. Images of H&E and immunohistochemical staining against TGF-β1 and VEGFR2 of the submesothelial compact zone of peritoneum. Bar = 100 μm, × 100. B. Images of Masson staining of peritoneum. Bar = 50 μm, × 200. E, F. The graph shows the quantitative data of the thickness of the compact zone and collagen fibers accumulation in peritoneal membrane. G, H. Quantitative data of relative TGF-β1 and VEGFR2 positive area (n = 6 per group). I. Quantification of ultrafiltration capacity. J. Analysis of glucose transporter status by PET. K-M. Analysis of IL-1, IL-6, and TNF-α in peritoneal effluent. *P < 0.05; **P < 0.01; ***P < 0.001; ns, not significant. Abbreviations: NS, Normal Saline. PDF, Peritoneal Dialysis Fluid.

logic features of PD-associated PF found in patients with long-term PD [29]. Furthermore, we determined that STAT3 inhibitor BP-1-102 reduced the thickening of the subcutaneous area and the accumulation of collagen fibers, and reversed the upregulation of TGF-β1 and VEGFR2. In our study, PFKFB3 was upregulated in the HG-PDF-induced rat PF model. PFKFB3 inhibitor 3PO could also reduce the accumulation of collagen fibers and suppress the development of PF. These in vivo experiments highlighted the effect of STAT3 and hyperglycolysis in the progression of PF.

Angiogenesis is an important contributor to PF [30, 31]. Our Masson and H&E staining and immunohistochemical experiments indicated that HG-PDF could induce peritoneal angiogenesis in rats. BP-1-102 or 3PO significantly reduced vascular density and decreased the expression of VEGFR2 and TGF-β1, as well as thickening of the subperitoneal region. The mechanism of anti-fibrotic effects of targeting STAT3/PFKFB3 is multifaceted in the peritoneum. A recent study has demonstrated that cytokines with different functions are induced after inflammation in patients. In this study, we discovered that the sustained stimulation of HG-PDF caused peritoneal tissue damage accompanied by the upregulated expression of interleukin-1 and interleukin-6, and the level of interleukin-6 was also upregulated in the NS group. Importantly, we found that STAT3 was the primary factor mediating IL-6 function. BP-1-102 reversed the level of IL-1 and IL-6 in the peritoneal dialysis effluent of PF rats, and it simultaneously alleviated PF. However, 3PO reduced only the level of IL-1. TNF-α was unaffected by BP-1-102 or 3PO. The results suggested that IL-6 and IL-1 might interact with each other as part of a cytokine network that alters normal cytokine signaling and promotes adaptive immune responses, leading to PF [14, 28, 32].

Moreover, Mateijsen et al. has reported that PF is associated with angiogenesis and peritoneal ultrafiltration. During PD, the solutes are processed by diffusion and ultrafiltration. In our study, PET analysis was performed to detect the net ultrafiltration volume of the 90-minute dialysate and the concentration of glucose to evaluate the peritoneal transport capacity. In comparison to the normal saline group, rats in the PF group had a lower ultrafiltration volume and concentration of glucose in the 90-minute dialysis effluent, which indicated that HG-PDF caused impaired peritoneal transport function. Consistently, BP-1-102 or 3PO treatment increased the ultrafiltration volume and the concentration of glucose in the dialysate, suggesting that inhibiting STAT3 or hyperglycolysis could partially ameliorate ultrafiltration failure and improve impaired peritoneal transport function by HG-PDF. Together, our study in rats demonstrated that targeting STAT3/PFKFB3 could exert anti-fibrotic effects by regulating peritoneal inflammation, angiogenesis, and peritoneal ultrafiltration.

To further explore the mechanism of the crosstalk between STAT3 and hyperglycolysis in the EMT of peritoneal mesothelial cells, we used HMrSV5 cells in an in vitro study. We found high expression of glycolytic enzymes (LDHA, PKM2, PFKFB3) upon HG stimulation in HMrSV5 cells, while knockdown of STAT3 downregulated the hyperglycolysis and EMT in HMrSV5 cells cultured in HG. In addition, we proved that overexpressed STAT3 plays a similar role to high glucose in promoting EMT, which further indicates that the activation of STAT3 plays an important role in HG-induced mesothelial cell EMT and hyperglycolysis. Our previous studies also found that BP-1-102 attenuated EMT and restrained the level of AGEs and MGO (a byproduct of glycolysis) in HMrsV5 cells [19, 33]. Another study discovered that IL-6 activated STAT3 to enhance the expression of HK2 and PFKFB3 [23]. Glycolysis is also known to regulate the EMT of different cell types [34, 35]. It has been reported that hyperglycolysis, induced by long-term PD, is associated with MMT (mesothelial-to-mesenchymal transition, a cell-specific form of EMT in mesothelial cells) [7]. Furthermore, in HMrSV5 cells, 3PO reversed the expression of mesothelial cell EMT marker proteins (α-SMA and E-cadherin) by reducing the PFKFB3 expression induced by high glucose. Moreover, knockdown of STAT3 downregulated the expression of glycolytic enzymes in HMrSV5 cells cultured in HG. Collectively, these results confirmed that the STAT3/PFKFB3 signaling pathway was involved in the progression of PF.

In conclusion, our study suggested that HG/STAT3/PFKFB3 might promote the progression of PF through regulating pro-fibrosis and angiogenesis. Targeting the STAT3/PFKFB3 signaling pathway may be an approach to maintain peritoneal integrity during long-term PD therapy.

Acknowledgements

This study was financially supported by the Science Foundation of Anhui Province (No: 1808085MH249) and the Natural Science Foundation of China (No: 81900697).

Disclosure of conflict of interest

None.

Address correspondence to: Pei Zhang, Department of Nephrology, The First Affiliated Hospital of Anhui Medical University, Hefei 230032, Anhui, P.R. China. Tel: +86-0551-62922111; Fax: +86-0551-63633742; E-mail: zhangpei@ahmu.edu.cn

References

[1] Mortier S, Faict D, Schalkwijk CG, Lameire NH and De Vriese AS. Long-term exposure to new peritoneal dialysis solutions: effects on the peritoneal membrane. Kidney Int 2004; 66: 1257-1265.

[2] Aroeira LS, Aguilera A, Sánchez-Tomero JA, Bajo MA, del Peso G, Jiménez-Heffernan JA, Selgas R and López-Cabrera M. Epithelial to mesenchymal transition and peritoneal membrane failure in peritoneal dialysis patients: pathologic significance and potential therapeutic interventions. J Am Soc Nephrol 2007; 18: 2004-2013.

[3] Krediet RT. Ultrafiltration failure is a reflection of peritoneal alterations in patients treated with peritoneal dialysis. Front Physiol 2018; 9: 1815.

[4] Krediet RT and Struijk DG. Peritoneal changes in patients on long-term peritoneal dialysis. Nat Rev Nephrol 2013; 9: 419-429.

[5] Shi Y, Hu Y, Wang Y, Ma X, Tang L, Tao M, Qiu A, Zhuang S and Liu N. Blockade of autophagy prevents the development and progression of peritoneal fibrosis. Front Pharmacol 2021; 12: 724141.

[6] Raby AC, González-Mateo GT, Williams A, Topley N, Fraser D, López-Cabrera M and Labéta MO. Targeting Toll-like receptors with soluble Toll-like receptor 2 prevents peritoneal dialysis solution-induced fibrosis. Kidney Int 2018; 94: 346-362.

[7] Si M, Wang Q, Li Y, Lin H, Luo D, Zhao W, Dou X, Liu J, Zhang H, Huang Y, Lou T, Hu Z and Peng H. Inhibition of hyperglycolysis in mesothelial cells prevents peritoneal fibrosis. Sci Transl Med 2019; 11: eaav5341.

[8] Yu H, Lee H, Herrmann A, Buettner R and Jove R. Revisiting STAT3 signalling in cancer: new and unexpected biological functions. Nat Rev Cancer 2014; 14: 736-746.

[9] Bromberg J and Darnell JE Jr. The role of STATs in transcriptional control and their impact on cellular function. Oncogene 2000; 19: 2468-2473.

[10] Zheng C, Huang L, Luo W, Yu W, Hu X, Guan X, Cai Y, Zou C, Yin H, Xu Z, Liang G and Wang Y. Inhibition of STAT3 in tubular epithelial cells prevents kidney fibrosis and nephropathy in STZ-induced diabetic mice. Cell Death Dis 2019; 10: 848.

[11] Zhang Y, Lu W, Zhang X, Lu J, Xu S, Chen S, Zhong Z, Zhou T, Wang Q, Chen J and Liu P. Cryptotanshinone protects against pulmonary fibrosis through inhibiting Smad and STAT3 signaling pathways. Pharmacol Res 2019; 147: 104307.

[12] Ye S, Luo W, Khan ZA, Wu G, Xuan L, Shan P, Lin K, Chen T, Wang J, Hu X, Wang S, Huang W and Liang G. Celastrol attenuates angiotensin II-induced cardiac remodeling by targeting STAT3. Circ Res 2020; 126: 1007-1023.

[13] Bharadwaj U, Kasembeli MM, Robinson P and Tweardy DJ. Targeting janus kinases and signal transducer and activator of transcription 3 to treat inflammation, fibrosis, and cancer: rationale, progress, and caution. Pharmacol Rev 2020; 72: 486-526.

[14] Chen W, Yuan H, Cao W, Wang T, Chen W, Yu H, Fu Y, Jiang B, Zhou H, Guo H and Zhao X. Blocking interleukin-6 trans-signaling protects against renal fibrosis by suppressing STAT3 activation. Theranostics 2019; 9: 3980-3991.

[15] Wang Z, Li J, Xiao W, Long J and Zhang H. The STAT3 inhibitor S3I-201 suppresses fibrogenesis and angiogenesis in liver fibrosis. Lab Invest 2018; 98: 1600-1613.

[16] Xiang DM, Sun W, Ning BF, Zhou TF, Li XF, Zhong W, Cheng Z, Xia MY, Wang X, Deng X, Wang W, Li HY, Cui XL, Li SC, Wu B, Xie WF, Wang HY and Ding J. The HLF/IL-6/STAT3 feedforward circuit drives hepatic stellate cell activation to promote liver fibrosis. Gut 2018; 67: 1704-1715.

[17] Zhao J, Qi YF and Yu YR. STAT3: a key regulator in liver fibrosis. Ann Hepatol 2021; 21: 100224.

[18] Yang X, Bao M, Fang Y, Yu X, Ji J and Ding X. STAT3/HIF-1α signaling activation mediates peritoneal fibrosis induced by high glucose. J Transl Med 2021; 19: 283.

[19] Zhang P, Dai H and Peng L. Involvement of STAT3 signaling in high glucose-induced epithelial mesenchymal transition in human peritoneal mesothelial cell line HMrSV5. Kidney Blood Press Res 2019; 44: 179-187.

[20] Tomida M, Ohtake H, Yokota T, Kobayashi Y and Kurosumi M. Stat3 up-regulates expression of nicotinamide N-methyltransferase in human cancer cells. J Cancer Res Clin Oncol 2008; 134: 551-559.

[21] Cao C, Zhao G, Yu W, Xie X, Wang W, Yang R, Lv X and Liu D. Activation of STAT3 stimulates AHSP expression in K562 cells. Sci China Life Sci 2014; 57: 488-494.
[22] Lee H, Chin H, Kim H, Jung H and Lee D. STAT3-mediated MLST8 gene expression regulates cap-dependent translation in cancer cells. Mol Oncol 2020; 14: 1850-1867.
[23] Ando M, Uehara I, Kogure K, Asano Y, Nakajima W, Abe Y, Kawauchi K and Tanaka N. Interleukin 6 enhances glycolysis through expression of the glycolytic enzymes hexokinase 2 and 6-phosphofructo-2-kinase/fructose-2,6-bisphosphatase-3. J Nippon Med Sch 2010; 77: 97-105.
[24] Mejias M, Gallego J, Naranjo-Suarez S, Ramirez M, Pell N, Manzano A, Suñer C, Bartrons R, Mendez R and Fernandez M. CPEB4 increases expression of PFKFB3 to induce glycolysis and activate mouse and human hepatic stellate cells, promoting liver fibrosis. Gastroenterology 2020; 159: 273-288.
[25] Ferrantelli E, Liappas G, Keuning ED, Vila Cuenca M, González-Mateo G, Verkaik M, López-Cabrera M and Beelen RH. A novel mouse model of peritoneal dialysis: combination of uraemia and long-term exposure to PD fluid. Biomed Res Int 2015; 2015: 106902.
[26] González-Mateo GT, Pascual-Antón L, Sandoval P, Aguilera Peralta A and López-Cabrera M. Surgical techniques for catheter placement and 5/6 nephrectomy in murine models of peritoneal dialysis. J Vis Exp 2018; 56746.
[27] Li Z, Yan H, Yuan J, Cao L, Lin A, Dai H, Ni Z, Qian J and Fang W. Pharmacological inhibition of heparin-binding EGF-like growth factor promotes peritoneal angiogenesis in a peritoneal dialysis rat model. Clin Exp Nephrol 2018; 22: 257-265.
[28] Yang X, Yan H, Jiang N, Yu Z, Yuan J, Ni Z and Fang W. IL-6 trans-signaling drives a STAT3-dependent pathway that leads to structural alterations of the peritoneal membrane. Am J Physiol Renal Physiol 2020; 318: F338-F353.
[29] Mateijsen MA, van der Wal AC, Hendriks PM, Zweers MM, Mulder J, Struijk DG and Krediet RT. Vascular and interstitial changes in the peritoneum of CAPD patients with peritoneal sclerosis. Perit Dial Int 1999; 19: 517-525.
[30] Zhu X, Shan Y, Yu M, Shi J, Tang L, Cao H and Sheng M. Tetramethylpyrazine ameliorates peritoneal angiogenesis by regulating VEGF/Hippo/YAP signaling. Front Pharmacol 2021; 12: 649581.
[31] Kariya T, Nishimura H, Mizuno M, Suzuki Y, Matsukawa Y, Sakata F, Maruyama S, Takei Y and Ito Y. TGF-β1-VEGF-A pathway induces neoangiogenesis with peritoneal fibrosis in patients undergoing peritoneal dialysis. Am J Physiol Renal Physiol 2018; 314: F167-F180.
[32] Fielding CA, Jones GW, McLoughlin RM, McLeod L, Hammond VJ, Uceda J, Williams AS, Lambie M, Foster TL, Liao CT, Rice CM, Greenhill CJ, Colmont CS, Hams E, Coles B, Kift-Morgan A, Newton Z, Craig KJ, Williams JD, Williams GT, Davies SJ, Humphreys IR, O'Donnell VB, Taylor PR, Jenkins BJ, Topley N and Jones SA. Interleukin-6 signaling drives fibrosis in unresolved inflammation. Immunity 2014; 40: 40-50.
[33] Zhang P, Dai H and Peng L. AGEs induce epithelial to mesenchymal transformation of human peritoneal mesothelial cells via upregulation of STAT3. Glycoconj J 2019; 36: 155-163.
[34] Jiang Y, Han Q, Zhao H and Zhang J. Promotion of epithelial-mesenchymal transformation by hepatocellular carcinoma-educated macrophages through Wnt2b/β-catenin/c-Myc signaling and reprogramming glycolysis. J Exp Clin Cancer Res 2021; 40: 13.
[35] Dong P, Xiong Y, Konno Y, Ihira K, Kobayashi N, Yue J and Watari H. Long non-coding RNA DLEU2 drives EMT and glycolysis in endometrial cancer through HK2 by competitively binding with miR-455 and by modulating the EZH2/miR-181a pathway. J Exp Clin Cancer Res 2021; 40: 216.